AUSTRALIAN JOURNAL OF MECHANICAL ENGINEERING
2022, VOL. 20, NO. 3, 825–837
https://doi.org/10.1080/14484846.2020.1756182

Taylor & Francis
Taylor & Francis Group

ARTICLE

An extensive analysis of frequency and transient responses in S and C-shaped gears

S. H. Yahaya [a], M. S. Salleh [a], Kenjiro T. Miura [b], A. Abdullah [a], A. R. M Warikh [a] and Z. Jano [c]

[a]FakultiKejuruteraanPembuatan, UniversitiTeknikal Malaysia Melaka, Durian Tunggal, Malaysia; [b]Graduate School of Science and Technology, Shizuoka University, Shizuoka, Japan; [c]PusatBahasa Dan Pembangunan Insan, UniversitiTeknikal Malaysia Melaka, Durian Tunggal, Malaysia

ABSTRACT

Gears are crucial mechanical components and considerably used in consumer and industrial machinery. Gears can be grouped into five types namely spur, helical, rack and pinion, worm and bevel. Spur gear has been selected as a case model in this study mainly because it is one of the basic types of gear which can be easily constructed and fabricated. Spur gear tooth is designed using S and C-shaped transition curves. These curves are constructed using the G^2 parametric Said-Ball cubic curve and clothoid templates. The result demonstrates that the C-shaped gear model which consists of the natural frequency of0.7408 Hz and low onaverage and standard deviation of 1.00E-3 mm and 8.072E-3 mm offers the most affordable displacement when compared with S-shaped and existing gear models.

ARTICLE HISTORY
Received 24 January 2020
Accepted 8 April 2020

KEYWORDS
Said-Ball cubic curve; S and C-transition curves; spur gear; vibration; displacement

1. Introduction

Radzevich (2012) defined gears or represented curves area set of geometric shapes confined by uniform teeth. Srikanth, Jeevanantham, and Nirmal (2014) stated that teeth may also be shown as the progressive projections connected in the rotating shafts. Hirani (2014) and Stadtfeld (2001) noted that the invaluable function of gears is to transmit the force or torque but it is also beneficial in a rotary motion and power production. Yahaya (2015) also stated that gears and transmission are two inseparable terminologies. Gears comprise two basic forms namely circular and noncircular forms. Circular form design uses a particular circle while the noncircular form is otherwise (Dejnozkova and Dokladal 2004). The circular types are spur, helical, rack and pinion, worm and bevel gearswhereasconical and elliptical gears are the common types of noncircular. Matsuura, Hashimoto, and Okuno (2013) discovered that an involute or known as evolvent curves has been appreciably used in circular form design since the seventeenth century. This statement is in rhyme with Dooner (2012) where Euler (1707–1783) and Huygens (1629–-1695) invent the use of the involute curve in gears. Besides, noncircular gears or NCG utilise an evolute curve in designing its tooth profile. To gain a better understanding of involute and evolute curves, Fang et al. (2010) and Belyaev (2004) generally defined these curves as the creation of path or locus by some points known from tangent definition and centre of curvature.

Relatively, sound and noise are the output responses generated from an inseparable terminology of gear and transmission. These particular responses result from vibration between gear teeth as discussed by Palermo et al. (2010). By reviewing these responses, gear sound is pleasantly considered in comparison with the noise. Zhou, Sun, and Tao (2014) and Åkerblom (2001) showed noise as a transmission error that occurred at certain frequencies which may also contribute to a high level of vibration. A number of studies have focused on gear noise reduction (Paul and Bhole 2010; Ognjanović and Kostić 2012; Tuma 2009). Michalski, Pawlus, and Żelasko (2011)emphasised that tooth shape and surface, tooth size and thickness, gear material, the number of teeth and pressure angle are influencing gear noise. Sankar, Raj, and Nataraj (2010), Beghini, Presicce, and Santus (2006) and Åkerblom (2001) also stressed that tooth shape modification could be viewed as one of the considerable factors in gear noise reduction. Involute and evolute curves have been applied by Xianzhang (2011) as a preferable method for tooth shape modification.

However, the applicability of these curves in improving tooth shape is still insufficient. Babu and Tsegaw (2009) remarked that these curves especially involute types only focus on the approximation concepts or methods to increase their efficaciousness. Chebyshev approximation theory and interpolation technique are used by Higuchi et al. (2007), Yan, Wang, and Zhou (2014) and Wu, Yin, and Zhao (2013) to enable these involute curves to represent an equation or a polynomial form (useful for its shape preservation) while Reyes, Rebolledo, and Sanchez

CONTACT S. H. Yahaya saifudin@utem.edu.my

(2008) employed the tracing points method in constructing this curve. The intention of using these two methods is to have an aesthetic appearance (beauty and interactivity) in involute curve design.The separation technique between geometry definition and tool selection has been introduced by Kapelevich and Kleiss (2002) that is known as the direct design method in involute spur and helical gears. Kapelevich (2000) also identified the use of asymmetrical tooth profiles in the involute curve that offers a significant value where the vibration effect can be minimised. The smooth contact of involute gears can be generated using partial and ordinary differential equations as well as ease-off topology (related to the surface) (Litvin et al. 2005; Kolivand 2014). Numerous methods are also utilised in designing the profile of involute gear such as B-spline curve, non-uniform rational B-splines (NURBS) and sweep surface generation as described by Barone (2001) and Barbieri, Zippo, and Pellicano (2014). These methods enable the tooth shape design to be controlled more easily. Xiao et al. (2014) revealed an involute gear is also engaged withneurosciencesuch as neural network and genetic algorithm. Thus, the above description shows that an involute curve is a non-parametric form because of theseassociatedmethods. Figure 1 shows an example of an involute curve.

Mathematically, parametric form increases the degree of freedom (DOF) (or known as a set of independent parameters) (Martinsson et al. 2007). DOF is the most desirableparameterin shape design. Prvan (1997) claimed that smooth curves are only presentable when using this form and this claim is also supported by Kouibia and Pasadas (2000). The parametric form is widely applied for plane curves representation particularly in computer-aided design (CAD) or in geometric modelling. A flexible CAD model is also developed once the parametric form used to provide the modifications on the model is prepared easily (Alpers 2006).On top of that, this study focused on the use of parametric form in tooth shape design, especially for spur gear model.

Said-Ball cubic curve (SBCC) was a parametric form applied throughout this study. Said (1990) revealed that SBCC is a third-degree (cubic) polynomial curve that permits an inflection point and is also highly suitable for G^2 (curvature) blending application curves. Moreover, the procedures of controlling shape

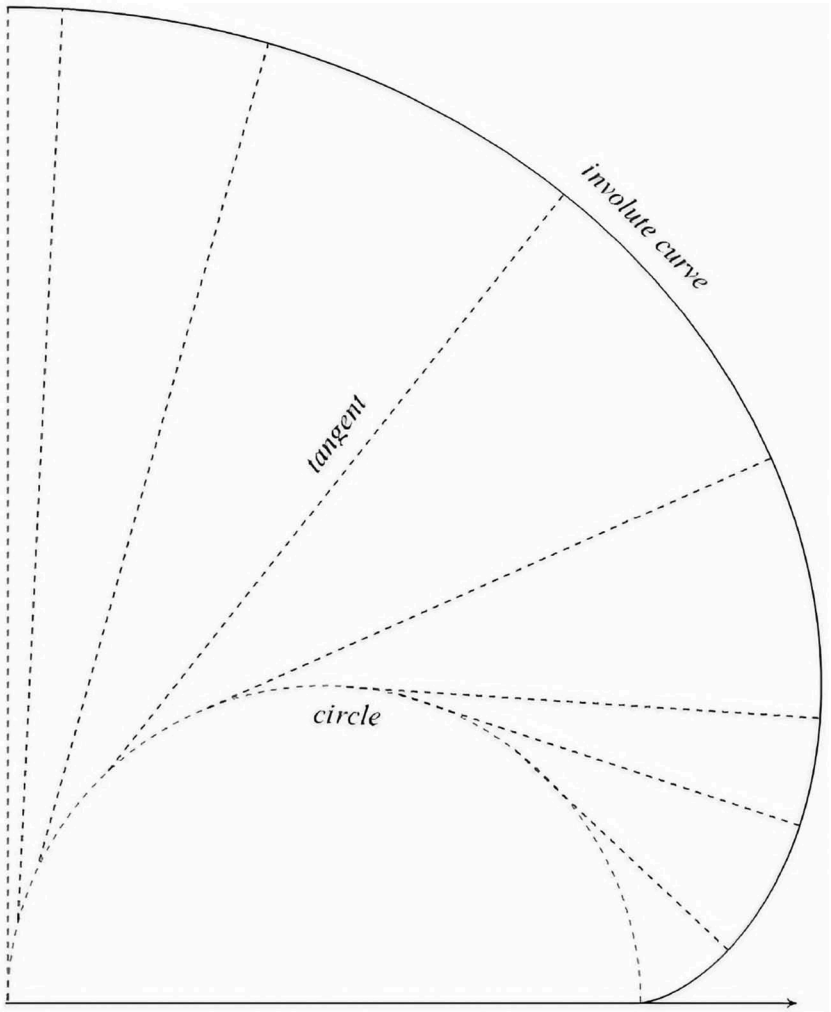

Figure 1. Involute curve design.

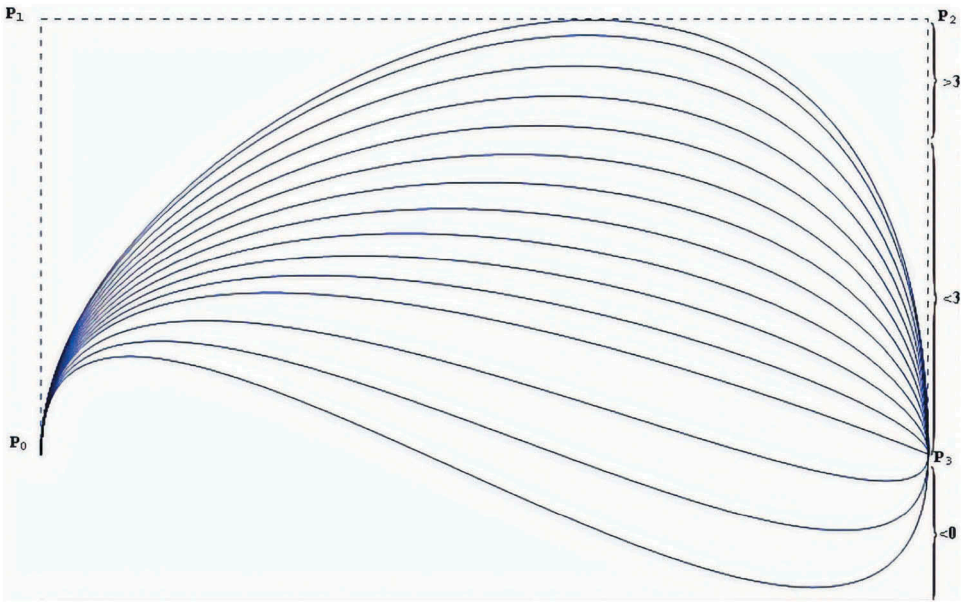

Figure 2. The influence of shape parameters in SBCC design.

or preserving curves become more effective because SBCC basis functions consist of two shape parameters, λ_0 and λ_1. Figure 2 shows these parameters' effectiveness. Meanwhile, Farin (2002) remarked that cubic Bézier curve (CBC) does not have any shape parameter. Therefore, the adjustment of control points is only applicable to its shape control of curve when applying this CBC. Ahmad (2009) reviewed the appearances of SBCC such as positivity curve, convex hull features, and geometric mapping suitability. Other uniqueness of shape parameters in SBCC can also represent several basis functions, namely, cubic Ball, CBC, and cubic Trimmer if the shape values are 2, 3 and 4.

Five cases of clothoid templates become a method of designing this parameterised curve by Baass (1984). Highway design was the first application using these templates which consisted of appearances such as the quality enhancement, users comfort, and safe driving and also the natural alignments which are designed to be in harmony with its surrounding areas. However, surprisingly, the outcomes are disastrous because of horizontal alignment (traditional approach) usage as shown by Baass (1984). Figure 3 shows the highway designed alignment models usingclothoid templates.

German Autobahn is a successful road network that deploys the clothoid templates (Zeller 2007). Vermeij (2000) asserted that clothoid curves were also usable in designing high-speed tracks, especially in railway designs. Shen et al. (2013) are in support of this statement in which they focused on a numerical study of cubic parabolas on the railway transition curves. These curves have the ability to identify the appropriatesuperelevationrate. The description of clothoid templates is proclaimed as follows: (1) To connect between a straight line and circle; (2) to connect between two circles with a C-transition (broken back); (3) to connect between two circles with an S-transition; (4) to connect between two straight lines and finally, (5) to connect between two circles with a C-transition (spiral) (Baass 1984; Walton and Meek 1996, 1999). Thus, the third and fifth cases of

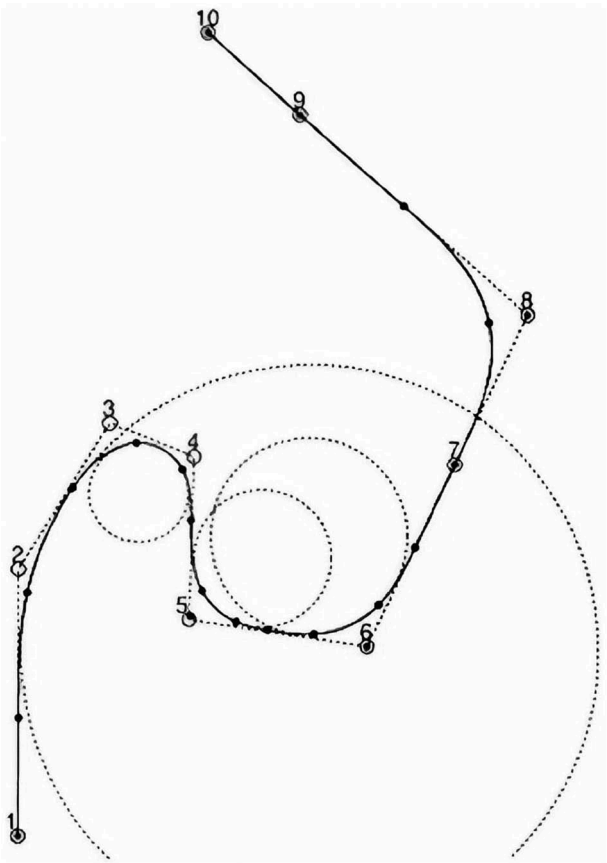

Figure 3. Highway design of alignment model using clothoid templates (Walton and Meek 1989).

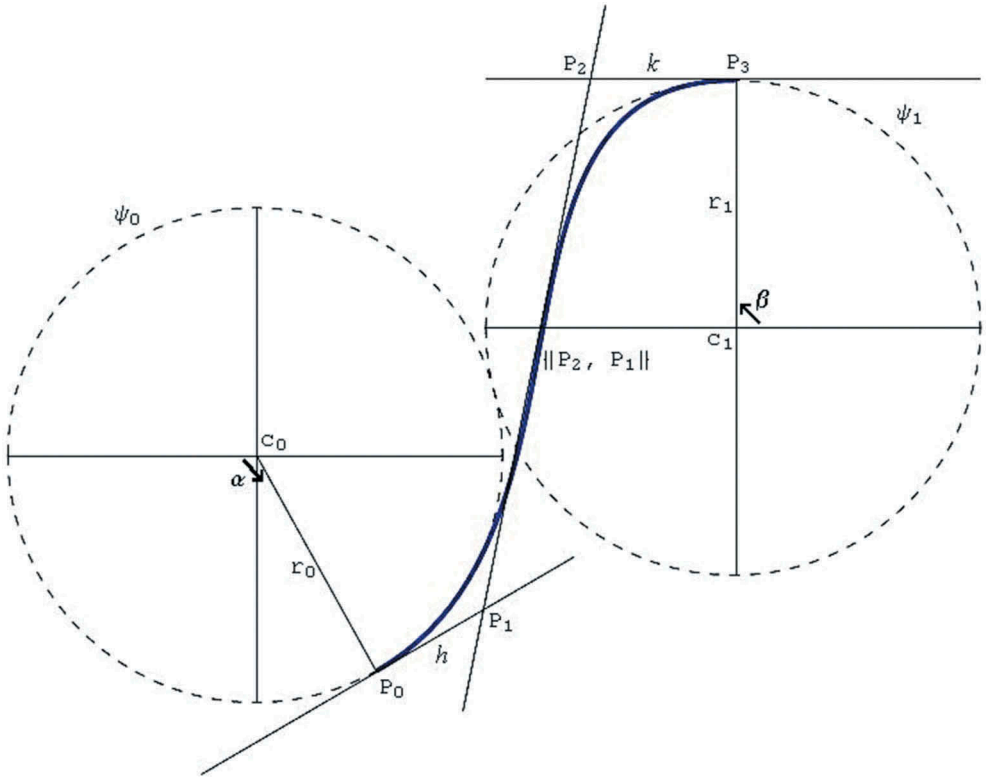

Figure 4. An S-shaped transition curve using SBCC.

clothoid templates are adopted by the dint of having a curve or profile similarity compared with an involute curve (existing profile) as shown in Figure 1.

The present study was to apply the parameterised curves (S and C-shaped transition curves) in spur gear design. These curves were designed using the third and fifth cases of clothoid templates and SBCC. The paper also proposed a spur gear model using frequency and transient modes analyses. Thus far, no comprehensive study has been conducted on the subject. In Section 2, the SBCCis reviewed including the definitions of notations and convections. The design of S and C-shaped transition curves is presented in Section 3 whereas the use of S and C-shaped transition curves in designing the spur gear model is included in Section 4. Numerous examples are also shown through the sections. Section 5 focuses on analysing of the proposed model using frequency and transient modes analyses. A short description of conclusions and recommendations for further study are remarked in Section 6.

2. Said-Ball cubic curve

Said-Ball cubic curve (SBCC), one of the new basis functions, was firstly introduced in Computer-Aided Geometric Design (CAGD) by Said (1990). Ali, Said, and Majid (1996) revisited the work of Said (1990) and offered a simple method to acquire the basis functions and its related developments. Consider a third-degree polynomial with its first-order derivative:

$$z(t) = a_0 + ta_1 + t^2a_2 + t^3a_3 \tag{1}$$

$$z'(t) = a_1 + 2ta_2 + 3t^2a_3 \tag{2}$$

with$t \in [0, 1]$. The endpoint and tangent conditions are given as:

$$z(0) = P_0,\ z(1) = P_3,\ z'(0) = \tau_0,\ z'(1) = \tau_1. \tag{3}$$

A blend with (1), (2) and (3) will construct

$$\begin{aligned} a_0 = P_0,\ a_0 + a_1 + a_2 + a_3 = P_3,\ a_1 \\ = \tau_0,\ a_1 + 2a_2 + 3a_3 = \tau_1. \end{aligned} \tag{4}$$

Simultaneous equation is used in (4) to yield

$$\begin{aligned} a_2 = 3P_3 - \tau_1 - 3P_0 - 2\tau_0,\ a_3 \\ = 2P_0 + \tau_0 - 2P_3 + \tau_1. \end{aligned} \tag{5}$$

Substitute (5) into (1) and re-write it using Hermite form to obtain

$$\begin{aligned} z(t) = (1 - 3t^2 + 2t^3)P_0 + t(1-t)^2\tau_0 + t^2(t-1)\tau_1 \\ + t^2(3 - 2t)P_3 \end{aligned} \tag{6}$$

Meanwhile, tangent condition can also be defined through

$$\tau_0 = \lambda_0(P_1 - P_0),\ \tau_1 = \lambda_1(P_3 - P_2) \tag{7}$$

The following form is produced when (6) and (7) are firmly fixed together:

$$z(t) = (1 - 3t^2 + 2t^3 - \lambda_0 t(1-t)^2)P_0 + \lambda_0 t(1-t)^2 P_1 + \lambda_1 t^2(1-t)P_2 + (t^2(3-2t) - \lambda_1 t^2(1-t))P_3 \quad (8)$$

Long division method and some simplifications in (8) are also used to express

$$z(t) = \phi_0(t)P_0 + \phi_1(t)P_1 + \phi_2(t)P_2 + \phi_3(t)P_3 \quad (9)$$

with

$$\phi_0(t) = (1-t)^2(1 + (2-\lambda_0)t), \phi_1(t) = \lambda_0(1-t)^2 t, \phi_2(t) = \lambda_1(1-t)t^2, \phi_3(t) = t^2(1 + (2-\lambda_1)(1-t)). \quad (10)$$

and P_0, P_1, P_2, P_3 are the control points where as $\phi_0(t), \phi_1(t), \phi_2(t), \phi_3(t)$ are the basic functions of this curve. Moreover, SBCC looks more presentable through the following form:

$$z(t) = (1-t)^2(1 + (2-\lambda_0)t)P_0 + \lambda_0(1-t)^2 tP_1 + \lambda_1(1-t)t^2 P_2 + t^2(1 + (2-\lambda_1)(1-t))P_3 \quad (11)$$

Relatively, the represented form in (11) is always delivered along with some general notations and convections. These general rules are useful in smoothing a plane curve. The Euclidean system consists of the vectors namely $A = < A_x, A_y >$ and $B = < B_x, B_y >$. The dot and cross products of these vectors are denoted such as $A \bullet B$ and $A\hat{B}$, respectively. Juhász (1998) and Artin (1957) expanded these products exemplifying that

$$A \bullet B = \|A\|\|B\| \cos(\theta) = A_x B_x + A_y B_y, \quad A\hat{B} = \|A\|\|B\| \sin(\theta) = A_x B_y - A_y B_x, \quad (12)$$

and where θ (or angle) is normally measured in anti-clockwise direction. Consider $z(t)$ defined as in (11), hence, its velocity (tangent) will be denoted by $z'(t)$ and the norm (speed) equals to

$$\|z'(t)\| = \sqrt{(x'(t))^2 + (y'(t))^2}. \quad (13)$$

Equation (13) is essentially associated to compute the arc length of a curve known as

$$S(t) = \int_a^b \|z'(t)\| dt. \quad (14)$$

Barnett (1985) claimed that the curve is regular (smooth) when using the parametric form and $z'(t) = 0$ consequently, the studies such as by Hoschek and Lasser (1993) and Faux and Pratt (1988) ensure the existence of curvature along the curve as follows

$$\kappa(t) = \frac{z'(t)\hat{z}''(t)}{\|z'(t)\|^3}. \quad (15)$$

$$\kappa'(t) = \frac{\varphi(t)}{\|z'(t)\|^5}, \quad (16)$$

with

$$\varphi(t) = \|z'(t)\|^2 \frac{d}{dt}\{z'(t)\hat{z}''(t)\} - 3\{z'(t)\hat{z}''(t)\}\{z'(t) \bullet z''(t)\}.$$

Equation (16) is an indicator to classify the plane curve into either spiral or transition feature when fulfiling certain conditions (will be further elaborated in Section 3). Jacobsen et al. (2006) supported this statement where they found that the aesthetic appearance between the curves can be seen upon the completion of plane curve classification. Costa (2002) agreed that the curve is productively smoothed because of the order derivatives used in (16). Besides, Lin (2009) also ensured that the order derivatives affect the shape of curves to be smoother and aesthetically pleasing. After knowing the SBCC with its related notations and convections, the descriptions of this paper continue on the design of transition curves.

3. Transition curve design

3.1. S-shaped transition curve using the third case of clothoid templates

Habib and Sakai (2003) revisited the work of Walton and Meek (1999) by giving the most desirable control points such as

$$P_0 = c_0 + r_0(\cos\alpha, \sin\alpha), \quad P_1 = P_0 + h(-\sin\alpha, \cos\alpha)$$
$$P_3 = c_1 - r_1(\cos\alpha, \sin\alpha), \quad P_2 = P_3 - k(-\sin\alpha, \cos\alpha) \quad (17)$$

wherec_0 and $c_1$knownas the centre points of circles ψ_0 and ψ_1, r_0 and r_1 are the radii of circles ψ_0 and ψ_1, h and k are the lengths or norms of $\|P_1, P_0\|$ and $\|P_3, P_2\|$, respectively, whereasα documented as an angle of circles rotated in anti-clockwise. These control points are unique only for an S-type (third case).

The adjustment of control points in (17) is essential to increase the degree of freedom and its applicability to construct

$$P_0 = c_0 - r_0(\cos\ \alpha, \sin\alpha), \quad P_1 = P_0 - h(-\sin\alpha, \cos\alpha)$$
$$P_3 = c_1 + r_1(\cos\beta, \sin\beta), \quad P_2 = P_3 + k(-\sin\beta, \cos\beta) \quad (18)$$

where the angles of circles ψ_0 and $\psi_1$are typified by α and β and also rotated in anti-clockwise. Other parameters are similar to (17). Moreover, the values of h and $k$are determined using the curvature continuity in (19). Figure 4 shows an S-shaped curve using SBCC.

$$\kappa(t=0) = -\frac{1}{r_0}, \quad \kappa(t=1) = \frac{1}{r_1}. \quad (19)$$

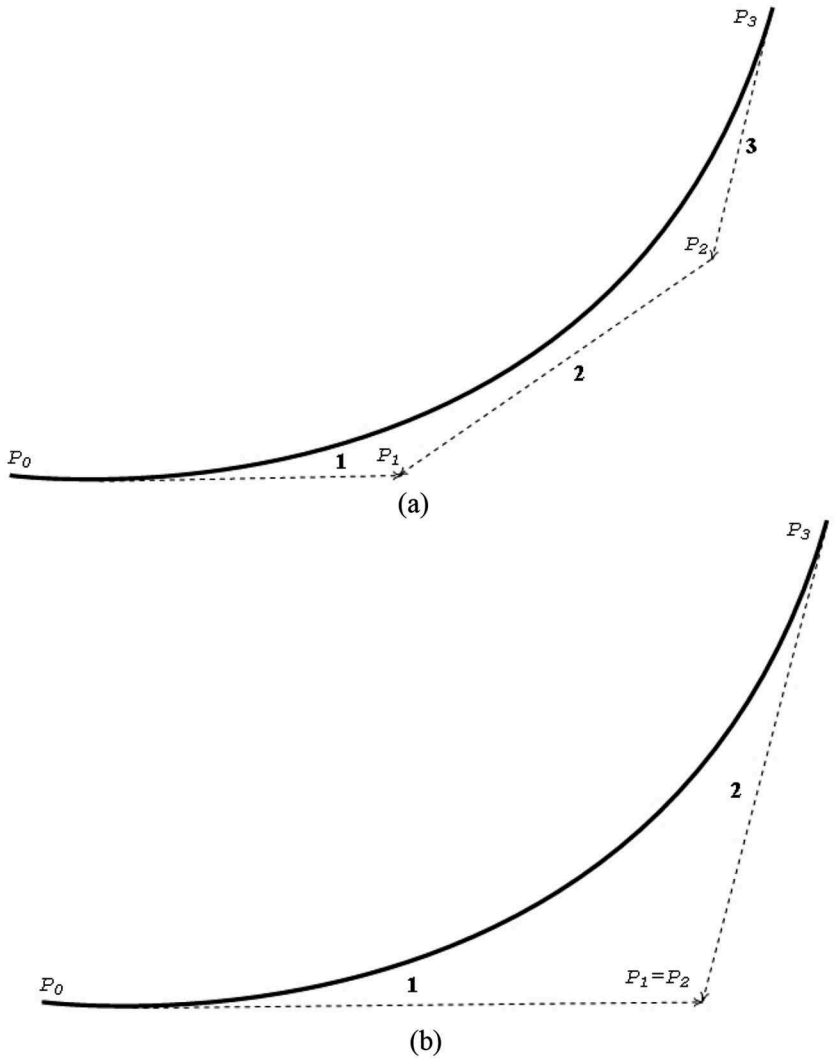

Figure 5. (a) Transition and (b) spiral curves segmentations.

3.2. C-shaped transition curve using the fifth case of clothoid templates

Baass (1984) found that the fifth case will produce a type of C-shaped transition curve as a single spiral. This finding is also supported by several studies by Habib and Sakai (2005) and Walton and Meek (1996) which focused on the G^2 spiral transition curve design between two circles. Relatively, the transition and spiral curve designsuse different segments. Figure 5 shows the designs of transition and spiral curves. It showed that three segments were applied for the C-shaped transition curve whereas only two segments were required in designing a C spiral curve (Walton, Meek, and Ali 2003).

The control points are stated as in Habib and Sakai (2003)

$$\begin{aligned} P_0 &= c_0 + r_0(\cos\alpha, \sin\alpha), \quad P_1 = P_0 + h(-\sin\alpha, \cos\alpha) \\ P_3 &= c_1 - r_1(\cos\beta, -\sin\beta), \quad P_2 = P_3 + k(\sin\beta, \cos\beta) \end{aligned} \tag{20}$$

The notations in (20) create a C-shaped transition curve that is applicable to the second case of clothoid templates (Baass 1984; Walton and Meek 1996, 1999). The design of fifth case template begins with the modifications of (20) where

$$\begin{aligned} P_0 &= c_0 - r_0(\cos\beta, \sin\beta), \quad P_1 = P_0 + k(\sin\beta, -\cos\beta) \\ P_3 &= c_1 + r_1(\cos\alpha, \sin\alpha), \quad P_2 = P_3 - h(-\sin\alpha, \cos\alpha) \end{aligned} \tag{21}$$

with c_0, r_0, β as the centre point, radius and angle of circle, ψ_0 whereas the centre point, radius and angle in circle, ψ_1 are denoted by c_1, r_1 and α. Parameters of$h$ and k are the length or norm of $\|P_3, P_2\|$ and $\|P_1, P_0\|$, respectively.

The segments used in (21) are also redefined by letting

$$P_1 = P_2. \tag{22}$$

Then, either h or k will be eliminated. If h is chosen, the expression in (22) will be simplified using a vector, $< \cos\alpha, \sin\alpha >$ to obtain

$$k = \frac{((c_1 - c_0) \bullet < \cos\alpha, \sin\alpha >) + r_1 + r_0\cos[\alpha - \beta]}{\sin[\beta - \alpha]}. \tag{23}$$

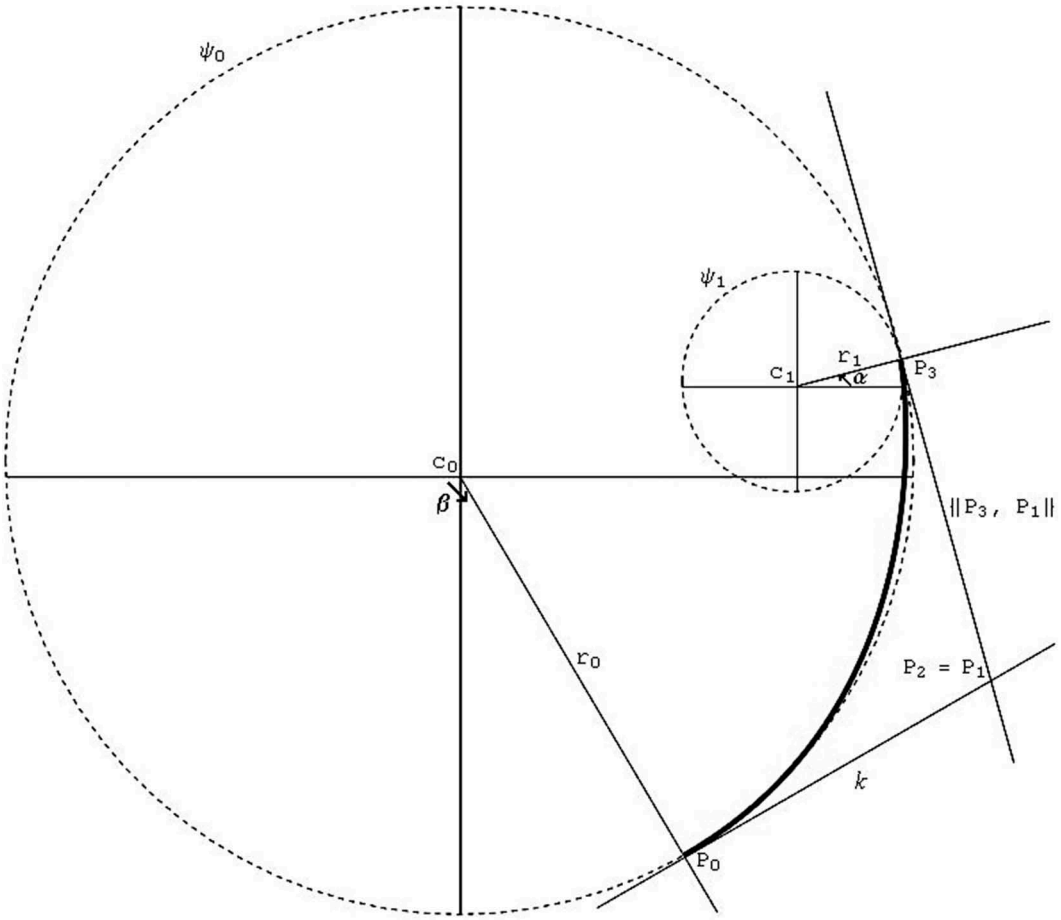

Figure 6. C-shaped transition curve using SBCC.

New control points that satisfy the fifth case template are given by

$$\begin{aligned} P_0 &= c_0 - r_0(\cos\beta, \sin\beta), \\ P_1 &= P_0 + k(\sin\beta, -\cos\beta), \\ P_3 &= c_1 + r_1(\cos\alpha, \sin\alpha). \end{aligned} \tag{24}$$

The following curvature continuity is applied for connecting a C-shaped curve between the two circles:

$$\kappa(t=0) = \frac{1}{r_0}, \quad \kappa(t=1) = \frac{1}{r_1}. \tag{25}$$

This continuity also calculates shape parameters values, λ_0 and λ_1 in (11). Figure 6 shows a C-shaped curve using SBCC.

4. Spur gear design model

4.1. S-shaped transition curve in spur gear tooth design

The design model commences with the geometric definition of clothoidtemplates constructed by adapting from Hwang and Hsieh (2007) study. This geometry is applied as a basic model in designing spur gear tooth. Figure 7 shows the geometry.

The tooth design process becomes easier when using the segmentation method. Two segments are needed to create the tooth using the S-shaped transition curve. This is because the S-shaped curve contains the starting point at the tangent of the base circle and the ending point at the tangent of the outside circle. For the first segment, the inputs consist ofc_0 = (−0.398, 0.689), c_1 = (0, 0.795), α = 0.6667π radian, β= 0.5π radian, r_0 = r_1 = 0.206 whereas in the second segment, the inputs arec_0 = (0.398, 0.689), c_1 = (0, 0.795), α = 0.3333π radian, β= 0.5π radian. Moreover, h and $k$are roughly equal to 0.2779 and 0.3780 using the above equations. Besides, the values of h and k are the same for both segments because of the symmetrical reason. Figure 8 displays the spur gear tooth design with its solid model using the S-shaped curve.

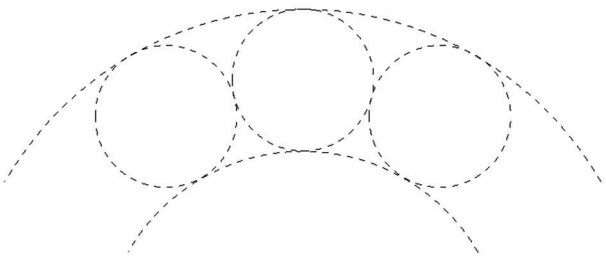

Figure 7. Geometric definition in clothoid templates.

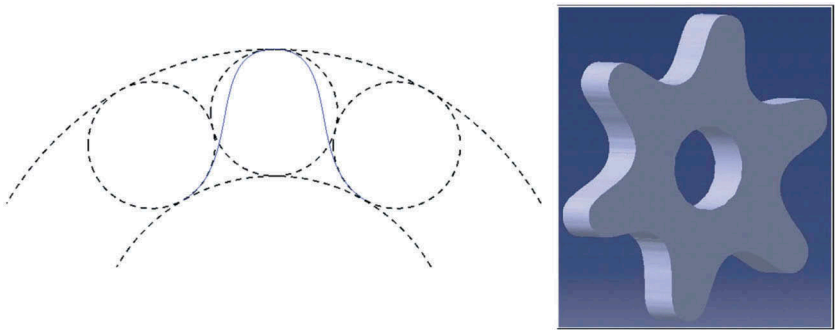

(a) (b)

Figure 8. (a) Spur gear tooth design and (b) its solid model using S-shaped transition curve.

4.2. C-shaped transition curve in spur gear tooth design

The elements in the fifth case template will be emerged by adapting Figure 7. The small circles are subsequently affixed to the big circles. Four segments are suitable for the tooth design using this case. Segment one consists of c_0 = (−0.398, 0.689), c_1 = (−0.247, 0.725), α = 0.05556π radian, β= 0.6667π radian, r_0 = 0.206 and r_1 = 0.05. Moreover, k= 0.1431 whereasλ_0 and $\lambda_1$are equal to 2.7695 and 0.3619, respectively. Segment two containsc_0 = (0, 0.795), c_1 = (−0.247, 0.725), β= 1.5π with k and shape parameters, λ_0, $\lambda_1$are computed as 0.2449, 2.1279 and 0.5343, respectively. Both segments possess a symmetrical curve or also known as mirroring or balancing the segments three and four. Du Sautoy (2009) supported this statement by stressing that the segments three and four have the same shape as compared with segments one and two. Figure 9 illustrates the spur gear tooth design with its solid model using a C-shaped curve.

The next section discusses the Dynamic response analysis of two models, S and C-shaped curves upon a completion of the spur gear solid model.

5. Dynamic response analysis

5.1. Normal modes analysis

Normal modes analysis was carried out to identify the natural frequency existed in particular models likeS and C-shaped curves. McConnell (1995) defined this natural frequency as the frequency which naturally vibrated after the motions are applied in the model or system. Natural frequency also occurs because of a model or system oscillation from the original position to anew position. This oscillation process takes more time without any outside interference such as damping. These positions change naturally. In general, natural frequency can be expressed through

$$fn = \frac{1}{2\pi}\sqrt{k} \tag{26}$$

where$m$ is the mass (kg) and k is the stiffness coefficient (N/m) (Blake 1961). Figure 10 shows the existing natural frequencies between the models and 10 modes implementations. As a result, S-shaped and the existing design (EM) have produced the highest natural frequency compared with the C-shaped model.

Figure 10 also depicts that the graph pattern of S-shaped and existing models is identical or in other

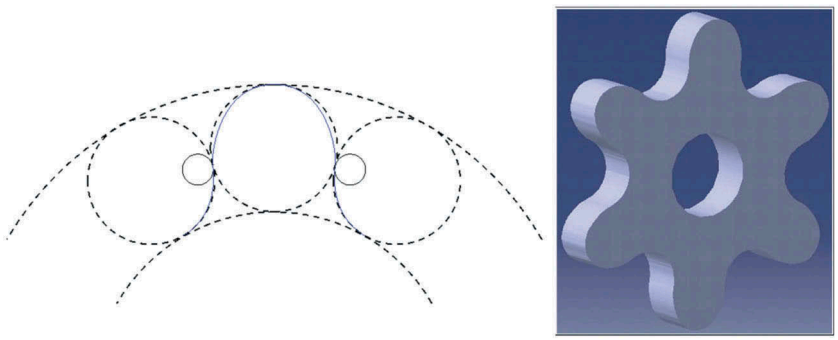

(a) (b)

Figure 9. (a) Spur gear tooth design and (b) its solid model using aC-shaped transition curve.

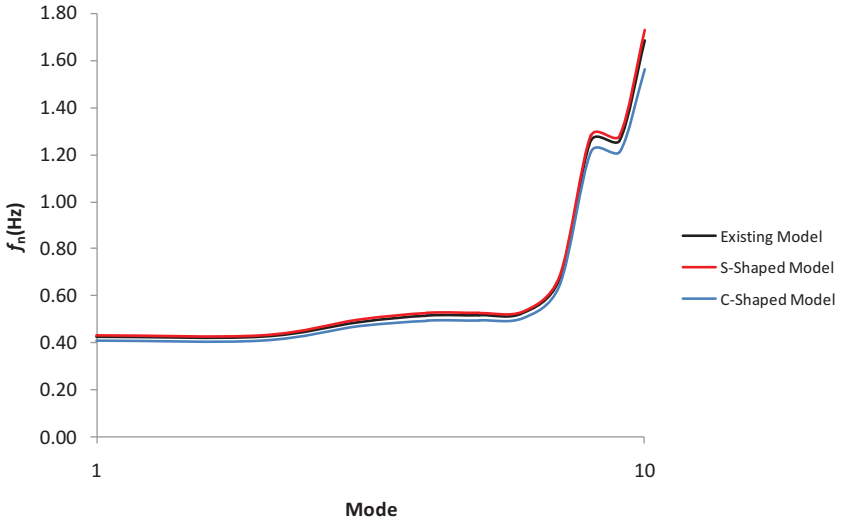

Figure 10. The natural frequencies amongst the models.

words, the existence of natural frequencies very similar. On average, the C transition model generated 0.7408 Hz whereas the S transition and EM produced 0.7926 Hz and 0.7769 Hz, respectively.

5.2. Frequency response analysis

Structural responses of the models in the frequency domain with the damping effect can be determined using the frequency response analysis. Numerous models or systems, for example, noise, vibration, rotary machinery, and transmission are predictable through this analysis. The frequency response analysis measures the outputs namely displacement, stress and force. However, displacement (δ) is very significant for the analysis because it is a the common vibration parameter to be computed (Klubnik 2008). The modal method is suitable for this frequency analysis because its solution is more reliable than the direct method. Fundamentally, the modal frequency response analysis originates from the following equation:

$$[M_n]\{\ddot{\alpha}_n\} + [C_n]\{\dot{\alpha}_n\} + [K_n]\{\alpha_n\} = \{l_n(t)\} \quad (27)$$

where$[M_n]\{\ddot{\alpha}_n\}$ is the matrix of mass, $[C_n]\{\dot{\alpha}_n\}$ is the matrix of damping, $[K_n]\{\alpha_n\}$is the matrix of stiffness and $\{l_n(t)\}$ is the loading vector (Komzsik 2009). However, the damping coefficient has been utilised in this modal frequency analysis (Table 1). Zehe, Gordon, and McBride (2002) asserted that stainless Steel Grade 304 or also known as AISI 304 has been widely used in numerous applications, namely, in gear

Table 1. AISI 304 and its characteristics (Peckner and Bernstein 1977).

Modulus of Elasticity	Yield Strength	Ultimate Strength	Poisson Ratio	Density	Damping Coefficient
195 GPa	215 MPa	505 MPa	0.29	8 gcc^{-1}	0.003

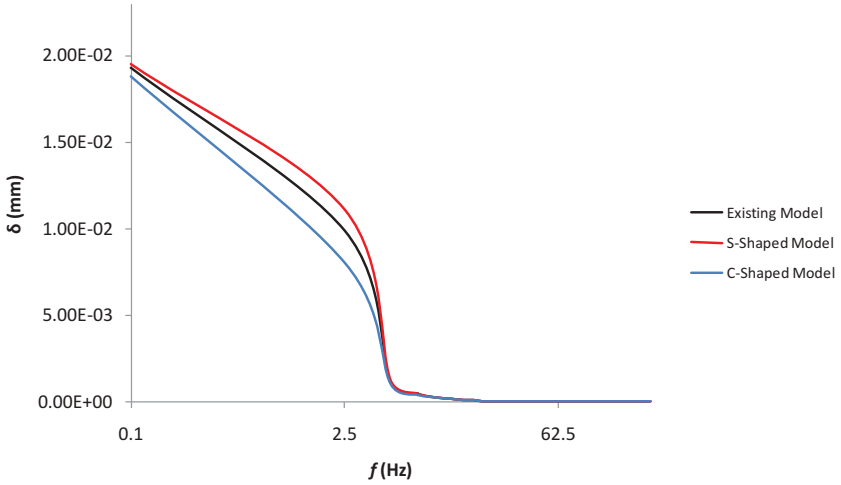

Figure 11. Modal frequency analysis in all models.

material. Table 1 shows the mechanical properties of AISI 304. Moreover, these properties are useful for this modal frequency analysis.

Figure 11 demonstrates the identified displacements in all models. Besides that, the frequency domain used is between the range of $f \in [0,250]$ with $\Delta f = 2.5$ Hz. Figure 11 also depicts that the blue colour (C-shaped) model has the minimum displacement (δ_{min} = 3.48E-7 mm) which does not occur in the S-shaped and EM models. Meanwhile, the S-shaped model produces maximum displacement where δ_{max} = 1.95E-2 mm. On average (δ_{mean}), the C-shaped model gives 1.00E-3 mm, followed by EM, 1.09E-3 mm and lastly, S-shaped is close to 1.15E-3 mm. From δ_{mean}, the S-shaped yielded higher displacement compared with the C-shaped model. Moreover, the high sound level was generated because the displacement was high as this statement was also supported by Bies and Hansen (2009), Brand and Schwab (2005) and Quinn (1987).

5.3. Transient response analysis

The response on the structural response models or systems with a real-time computing is the measurement derived after applying the transient or known as time analysis. The essentials of this analysis lookidenticaltothe frequency analysis excluding the time domain. The model of transient response analysis contains

$$[M_n]\{\ddot{\alpha}_n(t)\} + [C_n]\{\dot{\alpha}_n(t)\} + [K_n]\{\alpha_n(t)\} = \{l_n(t)\} \quad (28)$$

where all elements in (28) are identical to (27), including the independent variables, t (Hassan, Thanigaiyarasu, and Ramamurti 2008; Gomm 1987). The output parameter is still the same as δ in the time domain, $t \in [0,1]$ with $\Delta t = 0.05$ s. Figure 12 depicts the result of transient analysis in every model. Moreover, the blue colour model yielded the lowest graph pattern compared with others. Hence, surprisingly, the results hada close affinity between the transient and frequency analyses.

Figure 12 is being extensively discussed in the study. The results yielded that $t \in [0,1]$ with Δt = 0.05 s and the length of data, n = 20. Table 2 shows the statistical dispersion results between the models.

The δ_{mean} for C transition was 1.711E-2 mm, S transition was 1.838E-2 mm whereas EM was 1.808E-2 mm. According to Table 2, the C transition model portrayed the lowest displacement distribution within these three models. Moreover, the computation also focused on standard deviation (δμ) in every model. The results ofδμ for the EM was 8.332E-3 mm, S transition was 8.386E-3 mm and finally, δμ of C transition equalled to 8.072E-3 mm.

Levy (2011) found that a low standard deviation shows that the data points are very close to the mean or average whereas a high standard deviation expresses the data points which are spread out over the range. Therefore, the data distribution of C transition is definitely located to the nearest of its δ_{mean}; however, the S transition is otherwise. This may be attributed to the fact that δμ for C is smaller than EM and S transition models. This discussion may also answer any issue for the modal frequency analysis.

Based on the dynamic analyses, the C transition yielded the smallest dynamic displacement when compared with the S transition and EM models. Thus,

Table 2. The statistical dispersion between the models.

Statistical Items (mm)	EM	S Transition	C Transition
δ_{mean}	1.808E-2	1.838E-2	1.711E-2
δμ	8.332E-3	8.386E-3	8.072E-3
δ_{max}	2.706E-2	2.725E-2	2.632E-2
δ_{min}	0.000	0.000	0.000

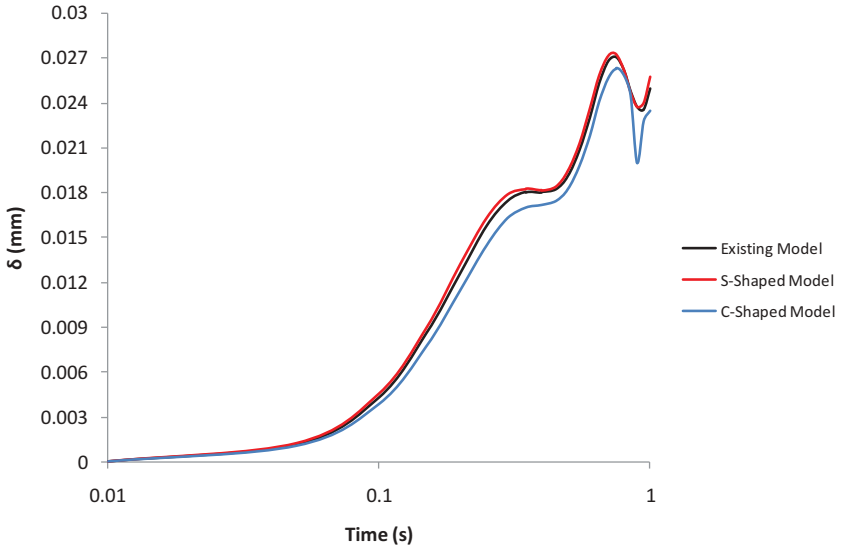

Figure 12. Transient frequency analysis in all models.

a low vibration will transmit through the gear model. This finding was supported by Bies and Hansen (2009) who develop an engineering noise control in theory and practice. Moreover, the noise or sound of gear will be significantly reduced by the C transition model utilisation.

6. Conclusion

In conclusion, this study utilises S and C-shaped transition curves to design spur gear teeth. These curves are constructed using the G^2 parametric Said-Ball cubic curve and clothoid templates. The S and C-shaped transition curves have been successfully used in re-designing a spur gear tooth model. The result shows that C-shaped gear model offers the most affordable displacement when compared with S-shaped and existing models because of their curvature profiles and derivatives are smoother when compared with S-shaped and EM (the use of fifth case template). Moreover, it is also verified that tooth profile modification is the main factor in reducing vibration in a very significant and consistent way.

For future study, unique features of C and S-transition curves can be further advanced particularly in acoustic response analysis. Once the transmission of low vibration is produced, noise is insignificant. The C and S-transition curves could also refine an aerodynamic model such as a car, high-speed train, and bullet. The velocity of the models or applications naturally becomes increasingly fast while the pressure is then depleted.

Acknowledgments

This study is supported by UniversitiTeknikal Malaysia Melaka. The authors gratefully acknowledge everyone who has contributed suggestions and comments.

Disclosure statement

No potential conflict of interest was reported by the authors.

Funding

This work was supported by the Universiti Teknikal Malaysia Melaka [FRGS/1/2018/TK03/UTEM/02/1].

ORCID

S. H. Yahaya http://orcid.org/0000-0003-0525-6243
M. S. Salleh http://orcid.org/0000-0003-4800-2470
Kenjiro T. Miura http://orcid.org/0000-0001-9326-3130
A. Abdullah http://orcid.org/0000-0003-1777-6246
A. R. M Warikh http://orcid.org/0000-0003-0070-2726
Z. Jano http://orcid.org/0000-0001-9173-4197

References

Ahmad, A. 2009. "Parametric Spiral and Its Application as Transition Curve." Ph.D. Thesis, UniversitiSains Malaysia.

Åkerblom, M. 2001. *Gear Noise and Vibration - A Literature Survey*. Stockholm, Sweden: Maskinkonstruktion.

Ali, J., H. Said, and A. Majid. 1996. "Shape Control of Parametric Cubic Curves." In *SPIE, Fourth International Conference on Computer-Aided Design and Computer Graphics*, edited by J. Zhou, 128–133. China.

Alpers, B. 2006. "Mathematical Qualifications for Using a CAD Program." In *IMA Conference on Mathematical Education of Engineers*, edited by S. Hibberd and L. Mustoe. London: Loughborough, Engineering Council.

Artin, E. 1957. *Geometric Algebra*. New York: Interscience.

Baass, K. 1984. "The Use of Clothoid Templates in Highway Design." *Transportation Forum* 1: 47–52.

Babu, V., and A. Tsegaw. 2009. "Involute Spur Gear Template Development by Parametric Technique Using Computer Aided Design." *African Research Review* 3 (2): 415–429. doi:10.4314/afrrev.v3i2.43640.

Barbieri, M., A. Zippo, and F. Pellicano. 2014. "Adaptive Grid-size Finite Element Modeling of Helical Gear Pairs." *Mechanism and Machine Theory* 82: 17–32. doi:10.1016/j.mechmachtheory.2014.07.009.

Barnett, H. 1985. "Criteria of Smoothness." *Journal of the Institute of Actuaries* 112 (3): 331–367. doi:10.1017/S0020268100042189.

Barone, S. 2001. "Gear Geometric Design by B-spline Curve Fitting and Sweep Surface Modelling." *Engineering with Computers* 17 (1): 66–74. doi:10.1007/s003660170024.

Beghini, M., F. Presicce, and C. Santus. 2006. "Proposal for Tip Relief Modification to Reduce Noise in Spur Gears and Sensitivity to Meshing Conditions." *Gear Technology* 23 (2): 34–40.

Belyaev, A. 2004. *Plane and Space Curves. Curvature. Curvature-based Features*. Saarbrücken: Max-Planck-InstitutfürInformatik.

Bies, D., and C. Hansen. 2009. *Engineering Noise Control: Theory and Practice*. Florida: CRC Press.

Blake, R. 1961. *Basic Vibration Theory, Shock and Vibration Handbook*. 1st ed. New York: McGraw-Hill.

Brand, L., and E. Schwab. 2005. "General Science Note: The Rainbow Is All in Your Head." *Origins* 58: 45–56.

Costa, L. 2002. "Estimating Derivatives and Curvature of Open Curves." *Pattern Recognition* 35 (11): 2445–2451. doi:10.1016/S0031-3203(01)00212-6.

Dejnozkova, E. and Dokladal, P., 2004, Modelling of overlapping circular objects based on level set approach. In *International Conference Image Analysis and Recognition*, Berlin, Heidelberg: Springer Publisher, pp. 416-423.

Dooner, D. 2012. *Kinematic Geometry of Gearing*. New Jersey: John Wiley & Sons.

Du Sautoy, M. 2009. *Symmetry: A Journey into the Patterns of Nature*. New York: HarperCollins.

Fang, S., L. Wang, M. Komori, and A. Kubo. 2010. "Simulation Method for Interference Fringe Patterns in Measuring Gear Tooth Flanks by Laser Interferometry." *Applied Optics* 49 (33): 6409–6415. doi:10.1364/AO.49.006409.

Farin, G. 2002. *Curves and Surfaces for CAGD: A Practical Guide*. Massachusetts: Morgan Kaufmann.

Faux, I., and M. Pratt. 1988. *Computational Geometry for Design and Manufacture*. Chichester: Ellis Horwood.

Gomm, W. 1987. "Stability Analysis of Explicit Multirate Methods." *Mathematics and Computers in Simulation* 23 (1): 34–50. doi:10.1016/0378-4754(81)90005-7.

Habib, Z., and M. Sakai. 2003. "G^2 Planar Cubic Transition between Two Circles." *International Journal of Computer Mathematics* 8: 959–967.

Habib, Z., Sakai, M., 2005. Family of G2 spiral transition between two circles. In: *Advances in Geometric Design*. John Wiley & Sons, Ltd., pp. 133–151.

Hassan, A., G. Thanigaiyarasu, and V. Ramamurti. 2008. "Effects of Natural Frequency and Rotational Speed on Dynamic Stress in Spur Gear." *In:WorldAcademy of Science, Engineering and Technology* 36: 1279–1287.

Higuchi, F., S. Gofuku, T. Maekawa, H. Mukundan, and N. Patrikalakis. 2007. "Approximation of Involute Curves for CAD-system Processing." *Engineering with Computers* 23 (3): 207–214. doi:10.1007/s00366-007-0060-3.

Hirani, H. 2014. *Applications of Tribology*. Delhi, India: Lecture notes distributed in Tribology at Indian Institute of Technology.

Hoschek, J., and D. Lasser. 1993. *Fundamentals of Computer Aided Geometric Design*. (Translation by L. L. Schumaker). Massachusetts: A.K. Peters Wellesley.

Hwang, Y., and C. Hsieh. 2007. "Determination of Surface Singularities of a Cycloidal Gear Drive with Inner Meshing." *Mathematical and Computer Modelling* 45 (3): 340–354. doi:10.1016/j.mcm.2006.05.010.

Jacobsen, T., R. Schubotz, L. Höfel, and D. Cramon. 2006. "Brain Correlates of Aesthetic Judgment of Beauty." *Neuroimage* 29 (1): 276–285. doi:10.1016/j.neuroimage.2005.07.010.

Juhász, I. 1998. "Cubic Parametric Curves of Given Tangent and Curvature." *Journal of Computer Aided Design* 25 (1): 1–9. doi:10.1016/S0010-4485(97)00046-8.

Kapelevich, A. 2000. "Geometry and Design of Involute Spur Gears with Asymmetric Teeth." *Mechanism and Machine Theory* 35 (1): 117–130. doi:10.1016/S0094-114X(99)00002-6.

Kapelevich, A., and R. Kleiss. 2002. "Direct Gear Design for Spur and Helical Involute Gears." *Gear Technology* 19 (5): 29–35.

Klubnik, R. 2008. "Measuring Displacement Using Accelerometers." *Maintenance Technology* 21 (3): 30–33.

Kolivand, A. 2014. "Involute Straight Bevel Gear Surface and Contact Lines Calculation Utilizing ease-Off Topography Approach." *SAE Technical Paper*, 1–1765.

Komzsik, L. 2009. *What Every Engineer Should Know about Computational Techniques of Finite Element Analysis*. 2nd ed. New York: CRC Press.

Kouibia, A., and M. Pasadas. 2000. "Smoothing Variational Splines." *Applied Mathematics Letters* 13 (2): 71–75. doi:10.1016/S0893-9659(99)00167-6.

Levy, J. 2011. *Your Options Handbook: The Practical Reference and Strategy Guide to Trading Options*. New Jersey: John Wiley & Sons.

Lin, H. 2009. "On the Derivative Formula of a Rational Bezier Curve at a Corner." *Applied Mathematics and Computation* 210 (1): 197–201. doi:10.1016/j.amc.2008.12.078.

Litvin, F., I. Gonzalez-Perez, A. Fuentes, K. Hayasaka, and K. Yukishima. 2005. "Topology of Modified Surfaces of Involute Helical Gears with Line Contact Developed for Improvement of Bearing Contact, Reduction of Transmission Errors, and Stress Analysis." *Mathematical and Computer Modelling* 42 (9): 1063–1078. doi:10.1016/j.mcm.2004.10.028.

Martinsson, H., F. Gaspard, A. Bartoli, and J. Lavest. 2007. "Reconstruction of 3D Curves for Quality Control." In *Image Analysis*, 760–769. Berlin, Heidelberg: Springer Publisher..

Matsuura, A., J. Hashimoto, and K. Okuno. 2013. "Geometric Visual Instruments Based on Object Rolling." In *Bridges 2013: Mathematics, Music, Art, Architecture, Culture*, 303–310. Netherlands: Tessellations Publishing.

McConnell, K. 1995. *Vibration Testing: Theory and Practice*. New Jersey: John Wiley & Sons.

Michalski, J., P. Pawlus, and W. Żelasko. 2011. "Surface Topography of Cylindrical Gear Wheels after Smoothing in Abrasive Mass, Honing and Shot Peening." *Journal of Physics* 311 (1): 012022. IOP Publishing.

Ognjanović, M., and S. Kostić. 2012. "Gear Unit Housing Effect on the Noise Generation Caused by Gear Teeth Impacts." *Strojniškivestnik-Journal of Mechanical Engineering* 58 (5): 327–337. doi:10.5545/sv-jme.2010.232.

Palermo, A., D. Mundo, A. Lentini, R. Hadjit, P. Mas, and W. Desmet. 2010. "Gear Noise Evaluation through Multibody TE-based Simulations: In." *Proceedings of International Conference on Noise and Vibration Engineering, Leauven, Belgium,*, 3033–3046.

Paul, I., and G. Bhole. 2010. "Modification of Spur Gear Using Computational Method-involutes Profile Being Modify." *2010 International Conference on Industrial Engineering and Operations Management*, 197–203. Dhaka, Bangladesh.

Peckner, D., and I. Bernstein. 1977. *Handbook of Stainless Steels*. New York: McGraw-Hill.

Prvan, T. 1997. "Smoothing Splines with Variable Continuity Properties and Degree." *Applied Mathematics Letters* 10 (2): 75–80. doi:10.1016/S0893-9659(97)00014-1.

Quinn, D. W. 1987. "A Finite Method for Computing Sound Propagation in Ducts." *Mathematics and Computers in Simulation* 29 (1): 51–64. doi:10.1016/0378-4754(87)90066-8.

Radzevich, S. 2012. *Dudley's Handbook of Practical Gear Design and Manufacture*. 2nd ed. London: Taylor & Francis Group.

Reyes, O., A. Rebolledo, and G. Sanchez. 2008. "Algorithm to Describe the Ideal Spur Gear Profile." *World Congress on Engineering (WCE) II*, London, U.K.

Said, H. 1990. "The Bézier-Ball Type Cubic Curves and Surfaces." *SainsMalaysiana* 19 (4): 85–95.

Sankar, S., M. Raj, and M. Nataraj. 2010. "Profile Modification for Increasing the Tooth Strength in Spur Gear Using CAD." *Journal of mechanical engineering Science* 2 (9): 740–749.

Shen, T., C. Chang, K. Chang, and C. Lu. 2013. "A Numerical Study of Cubic Parabolas on Railway Transition Curves." *Journal of Marine Science and Technology* 21 (2): 191–197.

Srikanth, N., A. Jeevanantham, and Nirmal. 2014. "Determination of Lock Slippage in Gear Tooth Using Quasi-static Analysis." *IOSR Journal of Mechanical and Civil Engineering (IOSR-JMCE)* 2(3): 19–22.

Tuma, J. 2009. "Gearbox Noise and Vibration Prediction and Control." *International Journal of Acoustics and Vibration* 14 (2): 99–108. doi:10.20855/ijav.2009.14.2242.

Vermeij, I. 2000. "Design of a High Speed Track." *HERON* 45 (1): 9–23.

Walton, D., and D. Meek. 1989. "Computer-aided Design for Horizontal Alignment." *Journal of Transportation Engineering* 115 (4): 411–424. doi:10.1061/(ASCE)0733-947X(1989)115:4(411).

Walton, D., and D. Meek. 1996. "A planar cubic Bézier spiral." *Journal of Computational and Applied Mathematics* 72 (1): 85–100. doi:10.1016/0377-0427(95)00246-4.

Walton, D., and D. Meek. 1999. "Planar G^2 Transition between Two Circles with a Fair Cubic Bezier Curve." *Computer Aided Design* 31 (14): 857–866. doi:10.1016/S0010-4485(99)00073-1.

Walton, D., D. Meek, and J. Ali. 2003. "Planar G^2 Transition Curves Composed of Cubic Bézier Spiral Segments." *Journal of Computational and Applied Mathematics* 157 (2): 453–476. doi:10.1016/S0377-0427(03)00435-7.

Wu, W., C. Yin, and S. Zhao. 2013. "New Involute Interpolation Method Based on Arc Length." *Computer Engineering and Design* 34 (1): 314–317.

Xianzhang, F. 2011. "Analysis of Field of Stress and Displacement in Process of Meshing Gears." *International Journal of Digital Content Technology and Its Applications* 5 (6): 345–357. doi:10.4156/jdcta.vol5.issue6.42.

Xiao, J., X. Deng, J. He, W. Ma, Y. Li, and J. Li. 2014. "Simulation and Analysis about Different Pressure Angle in Involute Gears Based on Neural Network." *Applied Mechanics and Materials 540*: 88–91.

Yahaya, S. 2015. "Said-Ball Cubic Transition Curve and Its Application to Spur Gear Design." Ph.D. Thesis, UniversitiSains Malaysia.

Yan, K., J. Wang, and R. Zhou. 2014. "A New Method of Point-to-point Comparison Interpolation for Involute." *Key Engineering Materials* 589: 708–711.

Zehe, M., S. Gordon, and B. McBride. 2002. *CAP: Computer Code for Generating Tabular Thermodynamic Functions from NASA Lewis Coefficients. NASA/TP–2001–210959/REV1*. Ohio, USA: Glenn Research Center.

Zeller, T. 2007. *Driving Germany: The Landscape of the German Autobahn*, 1930–1970. Vol. 5. New York: Berghahn Books.

Zhou, J., W. Sun, and Q. Tao. 2014. "Gearbox Low-noise Design Method Based on Panel Acoustic Contribution." *Mathematical Problems in Engineering* Article ID 850549, 10.